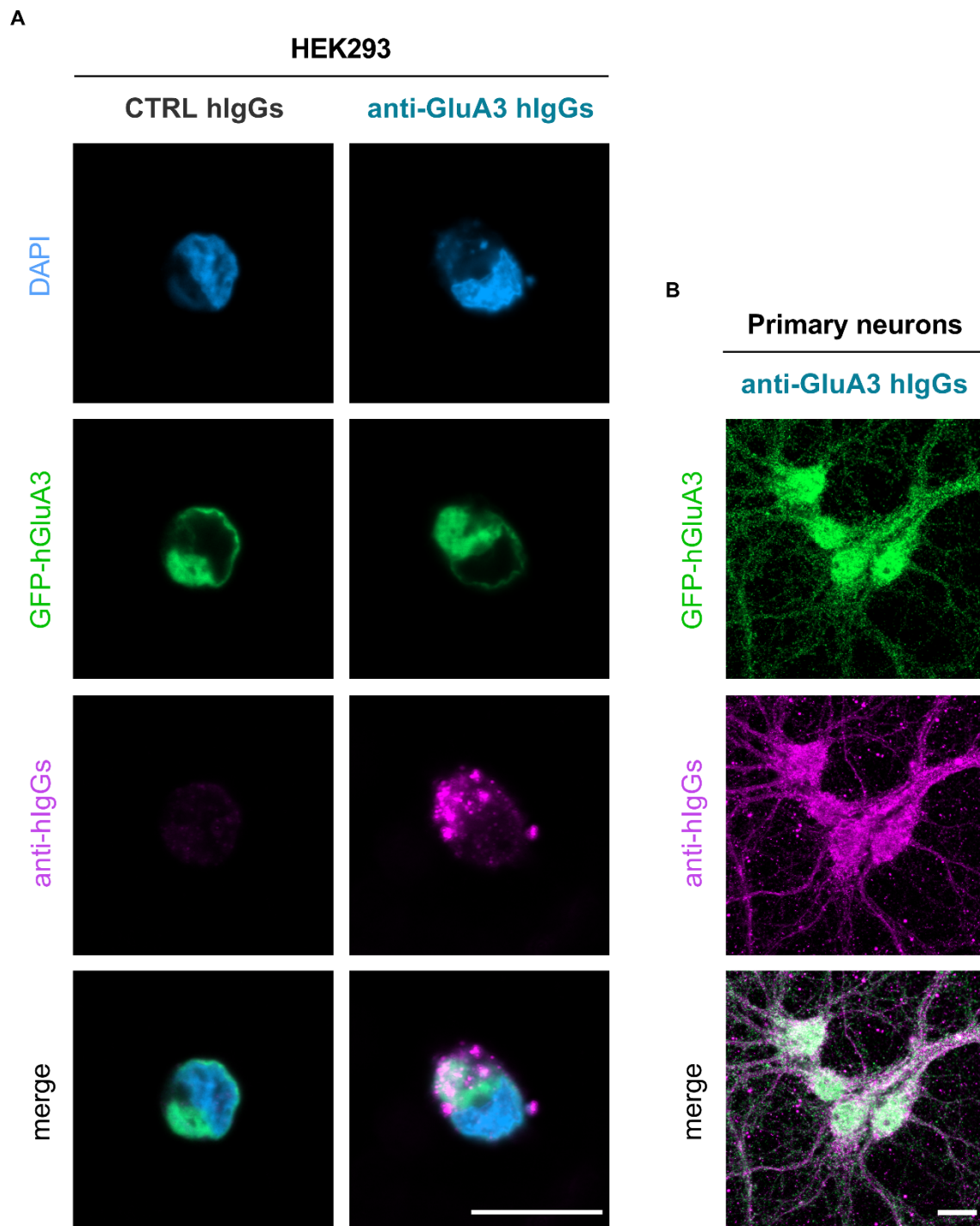


## **SUPPLEMENTAL FIGURES**

Fig. S1



**Fig. S1: Purified anti-GluA3 hlgGs and not CTRL hlgGs specifically bound over-expressed GFP-hGluA3 in both HEK293 cells and primary hippocampal neurons.** (A) Confocal images of HEK293 cells over-expressing human GluA3-GFP (green) and incubated with CTRL hlgGs (first column) or purified anti-GluA3 hlgGs (second column) for the staining of GluA3 (magenta channel). DAPI was used to recognize cell nuclei (blue channel). (B) Confocal images of primary rat hippocampal neurons overexpressing human GluA3-GFP

(green channel) and incubated with purified anti-GluA3 hIgGs for the staining of GluA3 (magenta channel). Merge panels are shown on the bottom of each column. Scale bar, 15 $\mu$ m.

**Fig. S2**

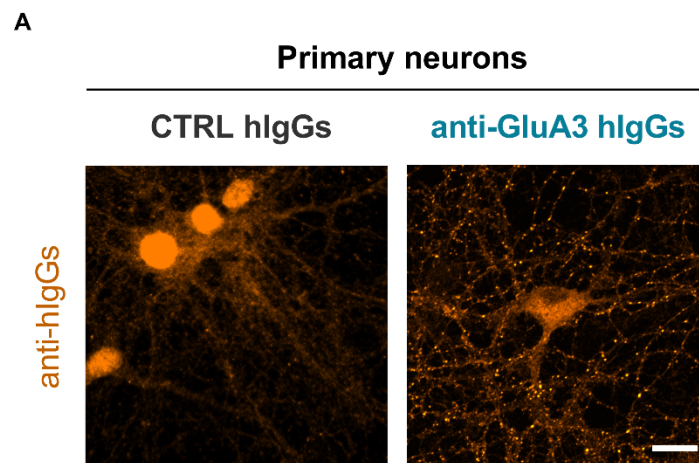


**Fig. S2: Purified anti-GluA3 hlgGs recognized endogenous GluA3 in primary hippocampal neurons.** (A) Confocal images of primary hippocampal neurons incubated with CTRL hlgGs (first column) or purified anti-GluA3 hlgGs (second column) for the staining of GluA3 (red channel). Scale bar, 15 $\mu$ m.

**Fig. S3**

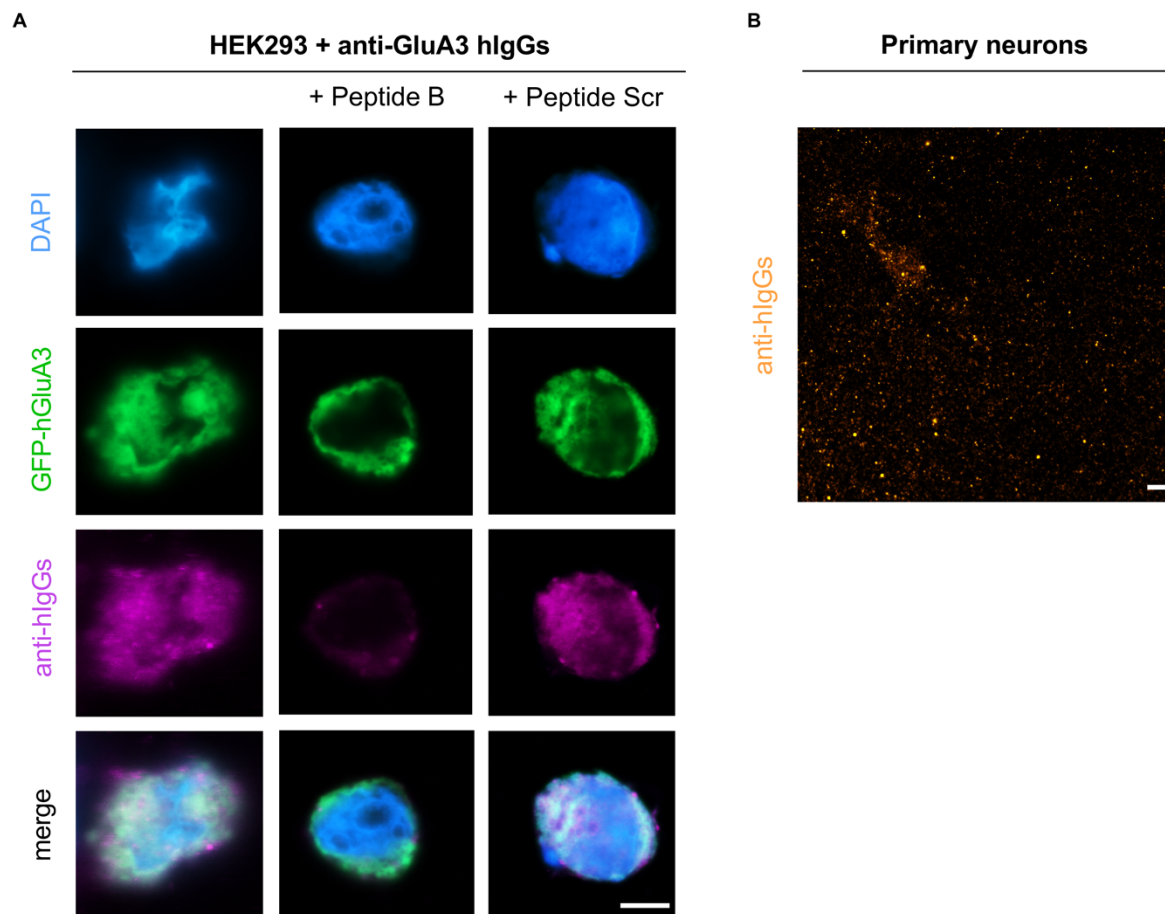


**Fig. S3: Purified anti-GluA3 hlgGs recognized GluA3 in live, unfixed, unpermeabilized HEK293 cells overexpressing GFP-hGluA3 and primary hippocampal neurons endogenously expressing GluA3.** (A) Confocal images of HEK293 cells over-expressing human GluA3-GFP (green channel) and incubated with purified anti-GluA3 hlgGs alone (first column), with purified anti-GluA3 hlgGs pre-incubated with *Peptide B* (second column) or with purified anti-GluA3 hlgGs pre-incubated with *Peptide Scramble* (third column) for the staining of GluA3 (magenta channel). DAPI was used to recognize cell nuclei (blue channel). Merge panels are shown on the bottom of each column. (B) Confocal images of primary rat hippocampal neurons incubated with purified anti-GluA3 hlgGs for the staining of GluA3 (red channel). Scale bar, 5 $\mu$ m.

**Fig. S4**

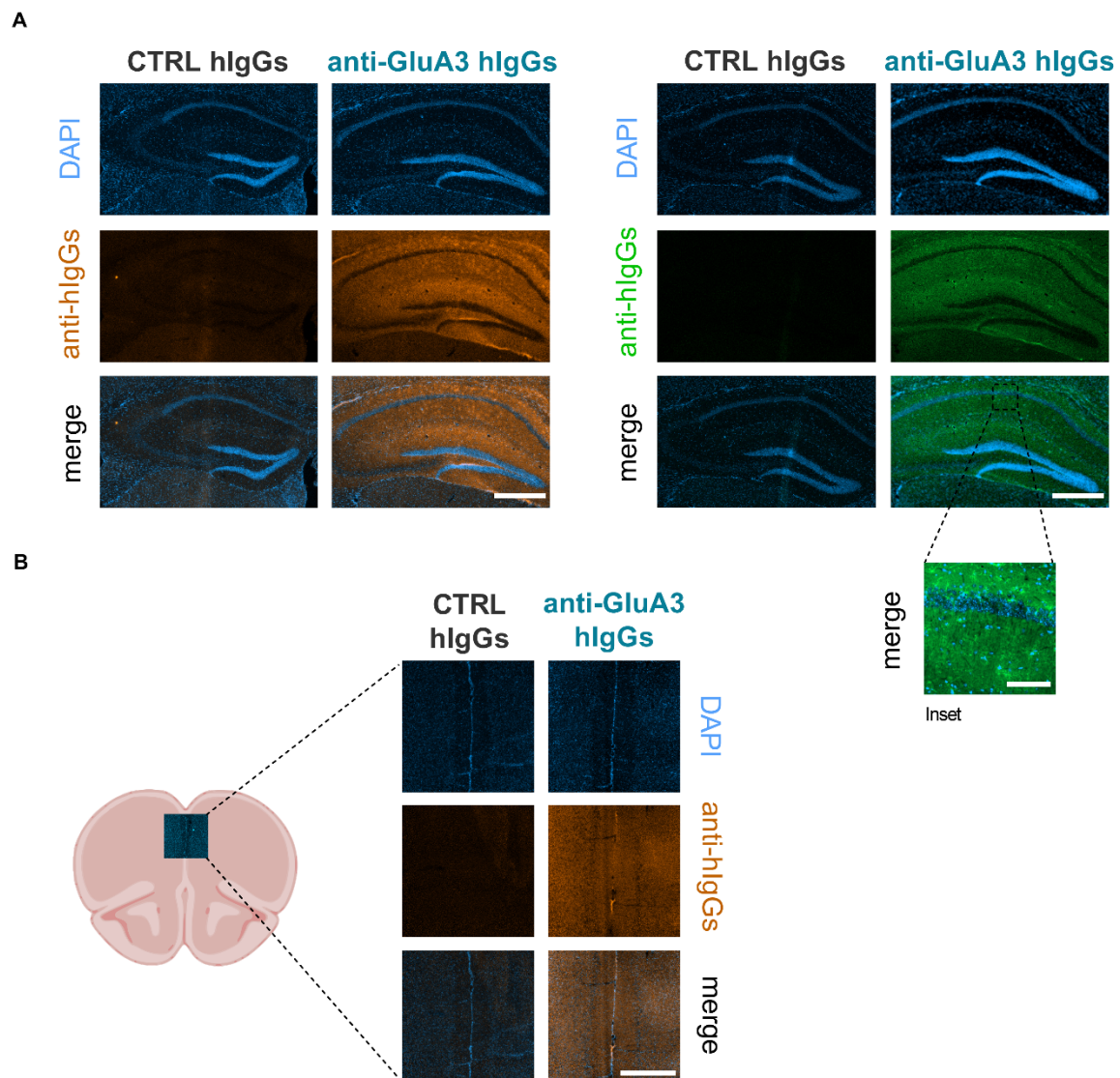


**Fig. S4: Detection of purified anti-GluA3 hlgGs but not CTRL hlgGs bound to mice's hippocampus and prefrontal cortex.** Immunostaining of human IgG (anti-hlgGs) in coronal brain sections of (A) hippocampus or (B) prefrontal cortex from mice infused with, alternatively, CTRL hlgGs (first columns) or purified anti-GluA3 hlgGs (second columns). In (A), the staining obtained using secondary anti-hlgGs conjugated to alternatively Alexa Fluor 555 (left block of images) and 488 (right block of images) is reported. In (A), the inset represents an image of the CA1 of anti-GluA3 infused animal with 20X magnification. In blue, DAPI signal is reported. Merge panels are shown on the bottom of each column. Scale bar, 500  $\mu$ m; inset scale bar, 100  $\mu$ m.

**Fig. S5**

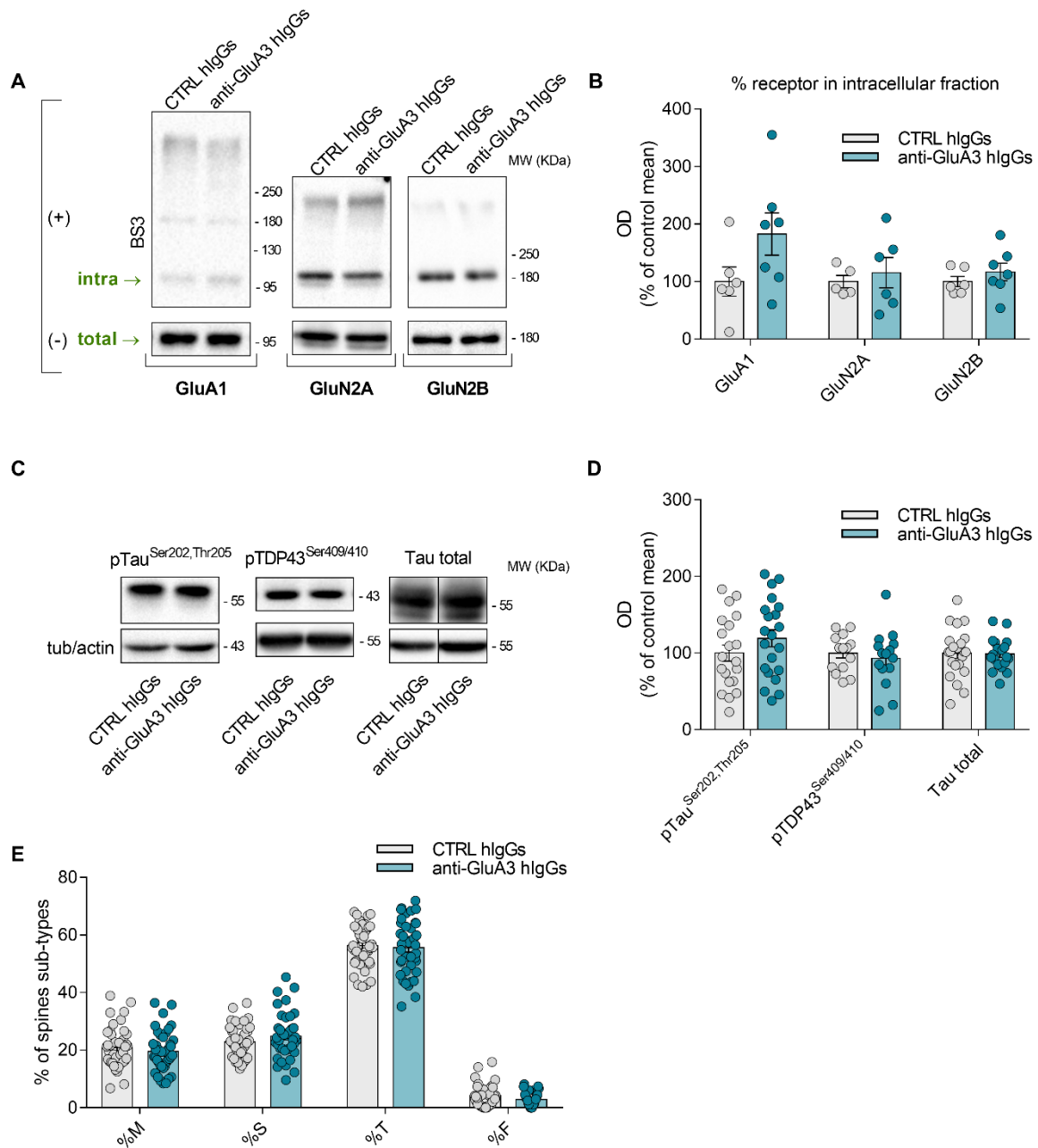


**Fig. S5: Anti-GluA3 hIgG administration did not affect surface GluA1, GluN2A, or GluN2B levels, total p-tau, pTDP43 or tau levels, or the relative percentages of spine subtypes in mouse PFC at the end of the chronic treatment.** (A) Western blot representative images and (B) bar graph of densitometric quantification of GluA1, GluN2A and GluN2B in intracellular fraction (from BS3 experiment, the blotted values represent the intracellular fraction band normalized on the total amount band) (two-tailed unpaired t-test; GluA1:  $t(11)=1.792$ ,  $p=0.1007$ ,  $n=6-7$ /group; GluN2A:  $t(9)=0.5023$ ,  $p=0.6275$ ,  $n=5-6$ /group; GluN2B:  $t(11)=0.9124$ ,  $p=0.3811$ ,  $n=6-7$ /group). (C) Western blot representative images and

(D) bar graph of densitometric quantification of p-Tau (Ser202, Thr205, AT8), pTDP43 (Ser409,410), and total Tau, in total homogenate obtained from mice PFC at the end of chronic treatment (two-tailed unpaired t-test; p-Tau:  $t(39)=1.258$ ,  $p=0.2160$ ,  $n=20-21$ /group; pTDP43:  $t(27)=0.5872$ ,  $p=0.5619$ ,  $n=14-15$ /group; Tau total:  $t(40)=0.1244$ ,  $p=0.9016$ ,  $n=22-20$ /group). (E) Proportions of different spine types in percentage of total spines: mushroom (M), stubby (S), thin (T) and filopodia (F) (two-tailed Mann-Whitney test or two-tailed unpaired t-test; % of M:  $t(81)=0.8363$ ,  $p=0.4054$ ,  $n=43-40$ /group; % of S:  $t(81)=1.338$ ,  $p=0.1847$ ,  $n=43-40$ /group; % of T:  $t(81)=0.3827$ ,  $p=0.7030$ ,  $n=43-40$ /group; % of F:  $U=660$ ,  $p=0.1344$ ,  $n=42-39$ /group). Bar graphs show mean  $\pm$  s.e.m. In (B), (D)  $n$  = number of animals; in (E),  $n$  = number of neurons. To apply two-tailed unpaired t-test, normal distribution was checked using D'Agostino & Pearson normality test.



**Fig. S6**

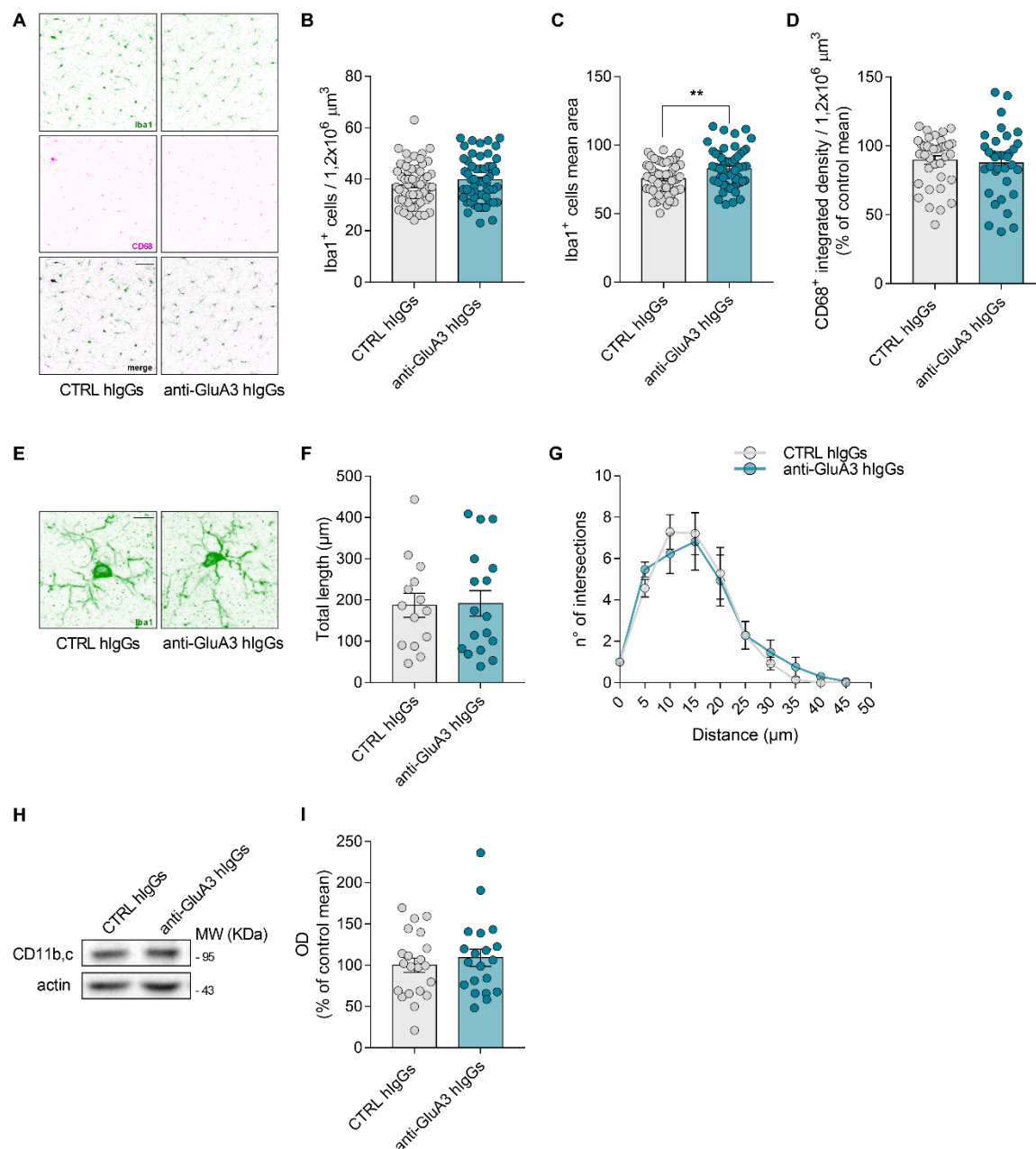


**Fig. S6: Effects of chronic anti-GluA3 hlgG administration on microglia.** (A) Representative images of Iba1 and CD68 staining in PFC slices at 20x magnification (scale bar = 50  $\mu\text{m}$ ). Iba1 staining quantification as (B) total number of Iba<sup>+</sup> cells (two-tailed unpaired t-test;  $t(115)=1.217$ ,  $p=0.2261$ ,  $n=60-57/\text{group}$ ) and (C) Iba1<sup>+</sup> cells mean area (two-tailed unpaired t-test;  $t(115)=3.126$ ,  $p=0.0022$ ,  $n=60-57/\text{group}$ ) in  $1.2 \times 10^6 \mu\text{m}^3$  of PFC slices. CD68 staining quantification as (D) integrated density of CD68 signal in  $1.2 \times 10^6 \mu\text{m}^3$  of PFC slices (two-tailed unpaired t-test;  $t(70)=0.4233$ ,  $p=0.6733$ ,  $n=37-35/\text{group}$ ). (E) Representative images of Iba1 staining in PFC slices at 63x magnification (scale bar = 10  $\mu\text{m}$ ); results of morphological Sholl analysis on Iba1 stained microglial arbor in PFC slices at 63x magnification expressed as (F) total length of ramifications (two-tailed unpaired t-test;

t(29)=0.1107, p=0.9126, n=14-17/group) and (G) complexity of arborization (multiple t-tests; df=29, p=ns, n=14-17/group). (H) Western blot representative images and (I) bar graph of densitometric quantification of CD11b,c (two-tailed unpaired t-test; t(39)=0.6781, p=0.5017, n=21-20/group) in total homogenate obtained from mice PFC at the end of chronic treatment with CTRL hIgGs and anti-GluA3 hIgGs. Bar graphs show mean  $\pm$  s.e.m. In (B), (C), (D), (F) and (G) n = number of images; in (I), n = number of animals. \*\*P < 0.01. To apply two-tailed unpaired t-test, normal distribution was checked using D'Agostino & Pearson normality test.

**Fig. S7**

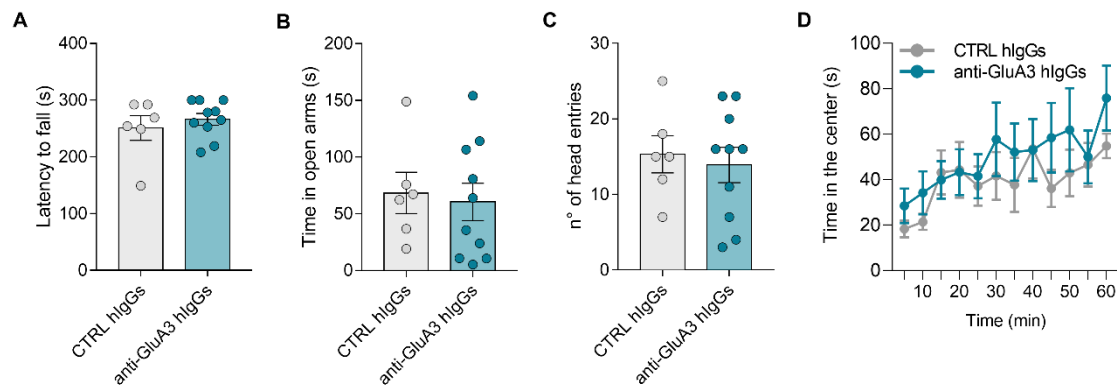


**Fig. S7: Chronic administration of anti-GluA3 hlgGs did not affect locomotor activity or motor coordination and did not trigger anxiety-like behaviour.** (A) Performance of mice in the rotarod task expressed as the latency to fall from the rotarod bar (two-tailed Mann-Whitney test;  $U=24$ ,  $p=0.5415$ ,  $n=6-10$ /group). Performance of mice in the Elevated Plus Maze expressed as (B) time spent in open arms (two-tailed unpaired t-test;  $t(14)=0.3052$ ,  $p=0.7647$ ,  $n=6-10$ /group) and (C) number of head entries (two-tailed unpaired t-test;  $t(14)=0.4012$ ,  $p=0.6944$ ,  $n=6-10$ /group). (D) Performance of mice in OF expressed as time spent in the centre (2way ANOVA; treatment:  $F(1,12)=0,6339$ ,  $p=0.4414$ ,  $n=6-8$ /group). Bar graphs show mean  $\pm$  s.e.m.  $n$  = number of animals. To apply two-tailed unpaired t-test, normal distribution was checked using D'Agostino & Pearson normality test or (when  $n$  insufficient) Shapiro-Wilk normality test.

**Fig. S8**

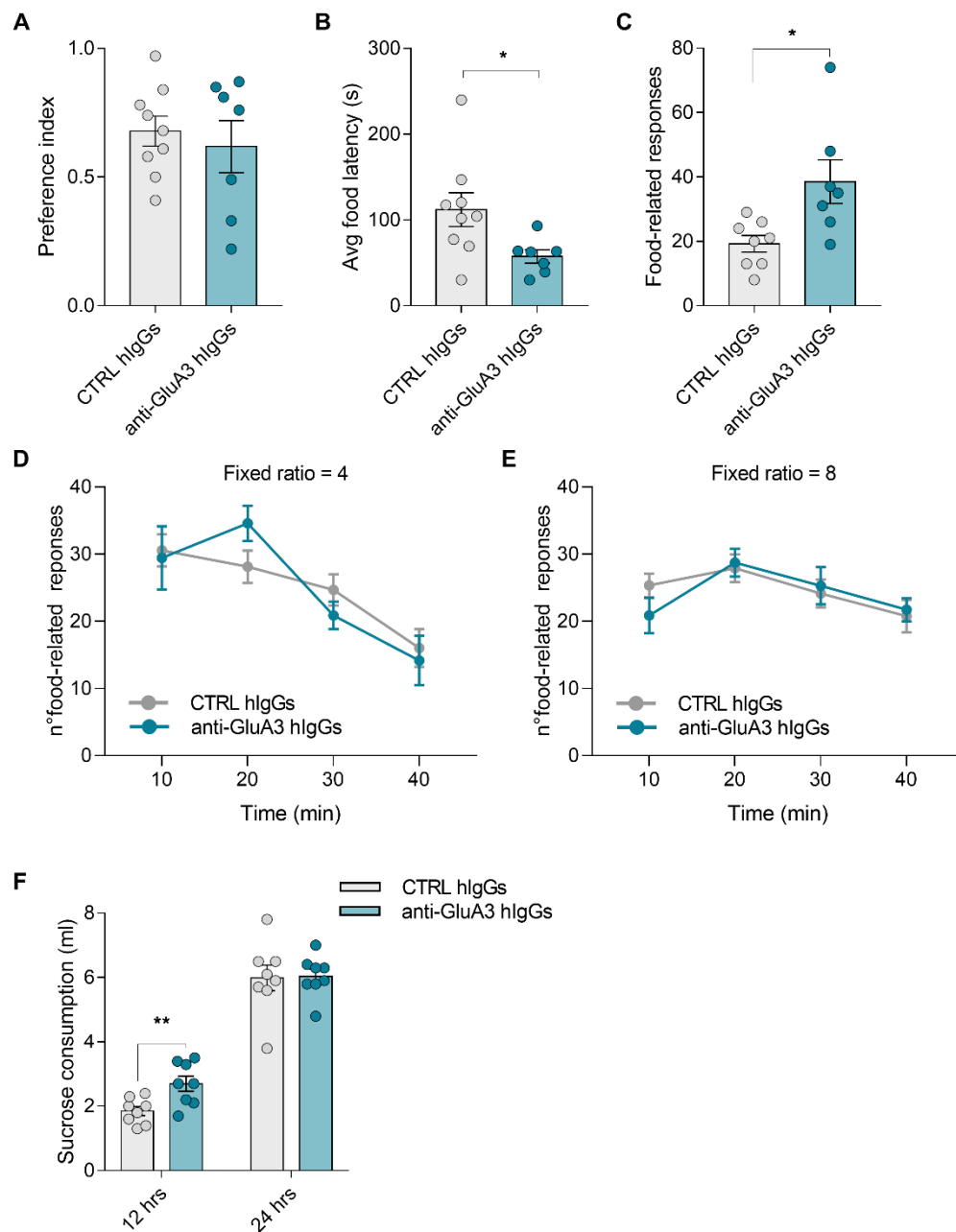


**Fig. S8: Chronic anti-GluA3 hlgG administration triggered binge-like eating and impulsivity.** Mice performance in the Food Seeking task without food restriction expressed as (A) preference index (two-tailed unpaired t-test;  $t(14)=0.5449$ ,  $p=0.5944$ ,  $n=9-7/\text{group}$ ), (B) average time between one food-related response and the subsequent one (i.e., avg food latency) (two-tailed unpaired t-test;  $t(14)=2.335$ ,  $p=0.0349$ ,  $n=9-7/\text{group}$ ) and (C) number of food-related responses (choice A) (two-tailed unpaired t-test;  $t(13)=2.789$ ,  $p=0.0153$ ,  $n=8-7/\text{group}$ ). Mice performance in the Food-Seeking task with food restriction and (D) fixed ratio = 4 (2way ANOVA; interaction:  $F(3,42)=1.383$ ,  $p=0.2613$ ,  $n=9-7/\text{group}$ ) or (E) fixed ratio = 8 (2way ANOVA; interaction:  $F(3,42)=1.209$ ,  $p=0.3184$ ,  $n=9-7/\text{group}$ ) expressed as number of food-related responses as a function of time. (F) Mice performance in the Sucrose Preference task

expressed as the sucrose consumption over a period of 12 or 24 hours (two-tailed unpaired t-test; 12 hours:  $t(14)=3.096$ ,  $p=0.0079$ ,  $n=8-8/\text{group}$ ; 24 hours:  $t(14)=0.1094$ ,  $p=0.9145$ ,  $n=8-8/\text{group}$ ). Bar graphs show mean  $\pm$  s.e.m.  $n$  = number of animals. \* $P < 0.05$ ; \*\* $P < 0.01$ . To apply two-tailed unpaired t-test, normal distribution was checked using D'Agostino & Pearson normality test or (when  $n$  insufficient) Shapiro-Wilk normality test.

**Fig. S9**

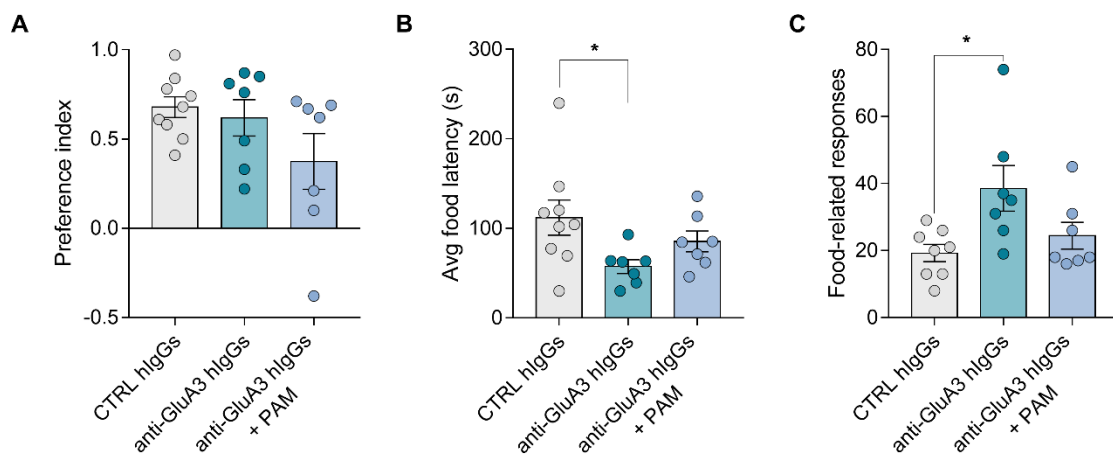


**Fig. S9: PAM administration partially rescued anti-GluA3 hlgG-mediated behavioural effects in a Food Seeking Task and under conditions of satiety.** Mice performance in the Food Seeking task without food restriction expressed as (A) preference index (ordinary one-way ANOVA; treatment:  $F(2,20)=2.292$ ,  $p=0.1270$ ,  $n=9-7-7$ /group; Tukey correction), (B) average of time between one food-related response and the subsequent one (ordinary one-way ANOVA; treatment:  $F(2,20)=3.29$ ,  $p=0.0582$ ,  $n=9-7-7$ /group; Tukey correction) and (C) number of food-related responses (ordinary one-way ANOVA; treatment:  $F(2,19)=4.625$ ,  $p=0.0231$ ,  $n=8-7-7$ /group; Tukey correction). Bar graphs show mean  $\pm$  s.e.m.  $n$  = number of animals. \* $P < 0.05$ . To apply one-way ANOVA, normal distribution was checked using Shapiro-Wilk normality test.